in the mean motion, is responsible for the sharp changes in the residual.

Remarks

This work presented the effects of the atmospheric drag and the Earth's oblateness on the volume of particles after an isotropic breakup. A special concern was given to the constriction points. The general nature of these points was not affected by the perturbations. However, it should be noted that the perturbations were considered as a field. It is sufficient for the J_2 part but is a limited particular model for the atmospheric perturbations. We have assumed this model because of its autonomous property. In other words, the perturbations here are an inherent part of the transition matrix as well as a part of the volume. Another way of modeling the atmospheric perturbations is by assuming a distribution of aerodynamic coefficients. This model cannot be handled by the current approach and may be carried out by using extensive numerical simulations for each particle.

References

[1] Jehn, R., "Dispersion of Debris Cloud from In-Orbit Fragmentation Events," *European Space Agency Journal*, Vol. 15, No. 1, 1991, pp. 63–77.

[2] Ashenberg, J., "On the Short-Term Spread of Space Debris," AIAA Paper 92-4441, Aug. 1992.

[3] Chobotov, V. A., "Dynamics of Orbiting Debris Cloud and the Resulting Collision Hazard to Spacecraft," International Academy of Astronautics, IAA-87-571, 1987.

[4] Jenkin, A. B., and Sorge, M. E., "Debris Cloud in Eccentric Orbits," AIAA Paper 90-3903, Sept. 1990.

[5] Ashenberg, J., "The Effect of the Earth's Oblateness on the Long-Term Dispersion of Debris," *Advances in Space Research* (to be published).

[6] Clohessy, W. H., and Wiltshire, R. S., "Terminal Guidance System for Satellite Rendezvous," *Journal of the Aerospace Sciences*, Vol. 27, Sept. 1960, pp. 653–658.

[7] Battin, R. H., *An Introduction to the Mathematics and Methods of Astrodynamics*, AIAA Education Series, AIAA, Washington, DC, 1987, pp. 450–455.

[8] Arnold, V. L., *Mathematical Methods of Classical Mechanics*, Springer-Verlag, Berlin, 1989, pp. 68–70.

Alfred L. Vampola
Associate Editor

Broadband Radio-Frequency Spectrum from Electrostatic Discharges on Spacecraft

H. C. Koons*
The Aerospace Corporation, Los Angeles, California 90009
and
T. S. Chin†
Lockheed Missiles & Space Company, Inc., Sunnyvale, California 94088

Introduction

VARIOUS aspects of the space environment can cause anomalous behavior of components on spacecraft. The plasma environment (especially around geosynchronous orbit) can differentially charge materials on the surface of a vehicle.[1–3] Spacecraft anomalies attributable to the resulting electrostatic discharges have been known to cause command errors, spurious signals, phantom commands, degraded sensor performance, part failure, and even complete mission loss.[4] Electromagnetic interference (EMI) from the resulting discharges may also interfere with communication systems on the spacecraft. Although many measurements of the properties of discharges have been made in space and in the laboratory, few have included the complete electromagnetic spectrum in the radio-frequency (RF) range. The purpose of this note is to compare new measurements of the RF spectrum from the Kapton blanket from the backside of the MILSTAR spacecraft's flexible substrate solar array (FSSA) with other space and laboratory data so that they will be more readily available for the analysis of spacecraft systems. The data may be used to estimate the effects of EMI from discharges on spacecraft systems operating in the frequency range from 100 kHz to 10 GHz.

Data

Figure 1 shows the broadband RF spectra of electrostatic discharges from 100 kHz to 10 GHz from a variety of different measurements. The original data have been converted to a standard distance of one meter. The MILSTAR flexible substrate solar array (FSSA) data were obtained from discharge measurements performed by Stanford Research Institute for Lockheed Missiles & Space Company, Inc. on a Kapton blanket sample from the backside of the solar array for the MILSTAR satellite. The blanket sample would cover eight solar cells arranged in a 2 × 4 array. The sample size was 15 × 30 cm (450 cm^2). About 20% of the Kapton blanket was covered on the inside by copper metallization. The data shown in Fig. 1 are from a series of tests on the sample at an electron beam energy of 20 keV and a beam current of 5 nA/cm^2. They are representative of the measurements at low frequency (LF), high frequency (HF), and uhf. The error brackets are drawn at ± 1 standard deviation for a sample of 14 or 15 discharges at each frequency.

The solid curve and the long-dashed curve are the spectra measured by Leung for two different-sized samples of Mylar.[5,6] The Mylar samples were irradiated by a 20-keV electron beam with a current density of 2–5 nA/cm^2. The peak pulse current was typically 150 A and the pulse width was 230 ns.

The measurement in Fig. 1 identified by the circle was made by the RF analyzer aboard the SCATHA spacecraft during a period when electron beam experiments were being performed on that vehicle? The RF analyzer measures electromagnetic emissions in the frequency range from 2 MHz to 30 MHz. The antenna for these measurements is an extendible 100-m, tip-to-tip dipole provided by the Goddard Space Flight Center for their dc-field experiment. The RF Analyzer can be operated in either a swept or a fixed-frequency mode. The design includes five frequency bands, two sweep rates, and two detection bandwidths. The signal amplitude is sampled 400 times per second, converted to an eight-bit digital format, and telemetered on a special purpose 3-kHz broadband data channel. During tape-recorded data collection, the amplitude is sampled 8 times per second. Only fixed frequency operation takes place in this mode. At the time the measurement in Fig. 1 was made, the RF analyzer was tuned to 20 MHz with a bandwidth of 4 kHz. The peak power was measured to be −83 dBm. It is not known what material was discharging. The electron beam was operating at 3 keV and 6 mA.

The dotted curve is the RF spectrum of a MIL-STD-1541A spark gap.[6] According to MIL-STD-1541A the spark gap is to be established at a level of 10 kV and the energy in the spark should be greater than 2×10^{-3} W-s.

The short-dashed curve is the spectrum measured by Wilson and Ma using a commercially available electrostatic discharge (ESD) simulator and a target: The target was an 8-mm-diam brass ball. For the spectrum shown in Fig. 1, the voltage was 4 kV. The peak current was 26 A with an approximate rise

Received March 4, 1993; revision received April 12, 1993; accepted for publication May 19, 1993.

*Senior Scientist, Space and Environment Technology Center, P. O. Box 92957. Member AIAA.

†Research Specialist, Space Systems Division, P. O. Box 3504.

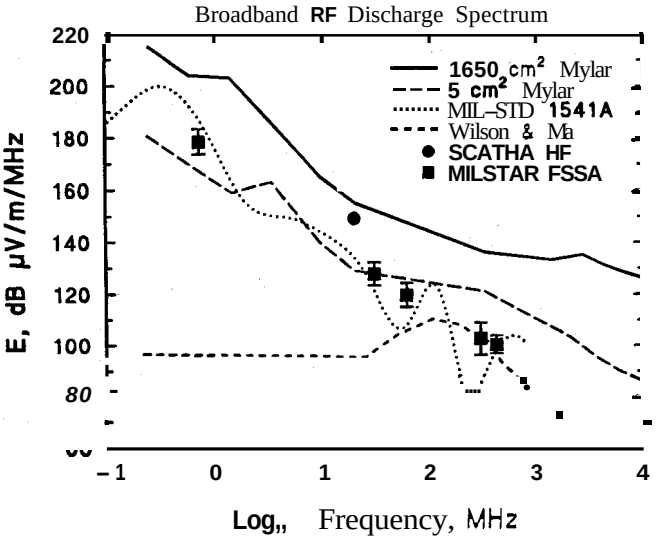

Fig. 1 Broadband RF discharge spectrum from laboratory and spacecraft measurements.

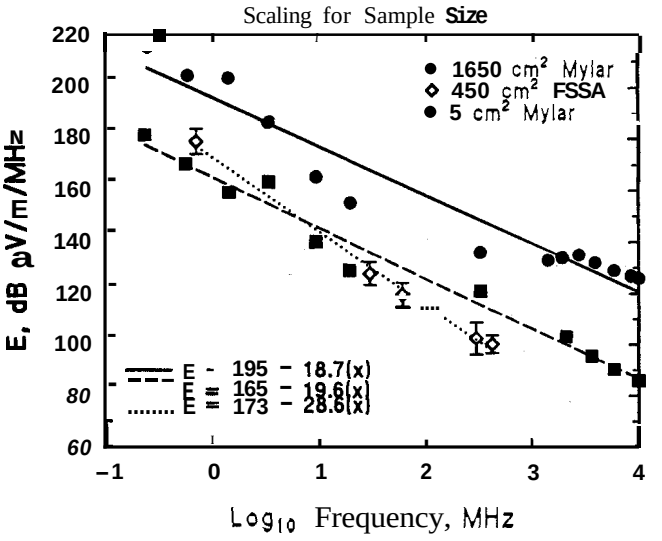

Fig. 2 A comparison of the spectrum from discharges on the MILSTAR FSSA blanket with linear regression fits to the large and small Mylar samples.

time of 0.9 ns and a width of about 2 ns. The short rise time and narrow width of this pulse account for the low electric-field levels below 10 MHz.

The data shown in Fig. 1 can be used to evaluate the possibility of EMI to spacecraft receivers from electrostatic discharges on spacecraft. However, the data from Wilson and Ma are not representative of spacecraft materials and should not be used in this application.

Area Scaling

Because the test samples used in the laboratory are often much smaller than the area of dielectric materials on spacecraft surfaces, it is important to determine how the spectra and intensities from such small samples scale to the spectra and intensities from larger samples. Leung measured the dependence of the peak discharge current on the area of the test sample for five sample sizes of Mylar from 5 cm^2 to 1650 cm^2 and found that the peak current varied as the area to the 0.4 power. The solid and dashed lines in Fig. 2 are the best-fitting straight lines to the electric-field spectra of the 5 cm^2 and the 1650 cm^2 Mylar samples, respectively, as obtained by a linear-regression analysis. These fits were made over the entire frequency range of Leung's measurements. For the 5 cm^2 sample, $E \propto f^{-0.98}$, and for the 1650 cm^2 sample, $E \propto f^{-0.94}$. Thus, the electric field is very nearly inversely proportional to the frequency over the entire frequency range. The dotted line in Fig. 2 is the best-fitting line for the MILSTAR FSSA Kapton sample for which we find that $E \propto f^{-1.48}$. Leung has published fits to the Mylar data for the frequency range below 30 MHz.[5] At those frequencies he finds that for the small sample, $E \propto f^{-1.5}$, and for the large sample, $E \propto f^{-1.8}$.

From Fig. 2, we find that the electric-field intensity from the large Mylar sample is 30 dB greater than the electric-field intensity from the small sample. The intensity ratio, then, is 32. Since the ratio of the areas is 330, the electric field scales as area to the 0.6 power.

The electric-field intensity from the MILSTAR FSSA Kapton blanket is not in accord with the area scaling for the Mylar. If the electric-field intensity was independent of the material, the intensity from the FSSA blanket would be about 23 dB higher than the intensity from the small Mylar sample. Instead, at frequencies above 10 MHz, it is actually lower than that from the small Mylar sample. Leung and Plamp have shown that the peak current and the pulse width of discharges are a function of beam energy and differ between Kapton and Mylar?

Since the spectral shape for the Kapton sample differs from that for the Mylar, and since the amplitude of the pulse from the Kapton differs from that expected from the area scaling derived from the Mylar samples, spectrum, amplitude, and scaling for other materials and for other sizes of Kapton is highly uncertain. Many factors must be taken into account when estimating the electric-field intensity from electrostatic discharges on such materials. We recommend that further research be conducted on spacecraft materials to accurately establish their discharge characteristics when they are used in a charging environment.

Acknowledgments

This work was supported by the Space and Missile Systems Center of the U. S. Air Force under Contract Nos. F04701-88-C-0089 and F04701-83-C-0025. We would like to thank W. Chang of Lockheed Missiles & Space Company, Inc., and T. Craven of Loral Space Systems for discussions of the data and R. Adamo at SRI, Inc. for his assistance in performing the tests on the MILSTAR samples.

References

'Fennell, J. F., Koons, H. C., Leung, M. S., and Mizera, P. F., "A Review of SCATHA Satellite Results: Charging and Discharging," ESA-SP-198, European Space Agency, Noordwijk, The Netherlands, 1983.

[2]Mullen, E. G., Gussenhoven, M. S., and Garret, H. B., "A Worst-Case Spacecraft Environment as Observed by SCATHA on 24 April 1979," AFGL-TR-81-0231, Air Force Geophysics Lab., Hanscom, MA, 1981.

[3]Mizera, P. F., and Boyd, G., "A Summary of Spacecraft Charging Results," *Journal of Spacecraft and Rockets*, Vol. 20, No. 5, 1983, pp. 438–443.

[4]Robinson, P. A., "Spacecraft Environmental Anomalies Handbook," GL-TR-89-0222, Air Force Geophysics Lab., Hanscom, MA, Aug. 1989.

[5]Leung, P. L., "Characteristics of Electromagnetic Interference Generated during Discharge of Mylar Samples," *IEEE Transactions* on *Nuclear Science*, Vol. NS-31, No. 6, 1984, pp. 1587–1590.

[6]Leung, P. L., "Characteristic of Electromagnetic Interference Generated by Arc Discharges," 9th Aerospace Testing Seminar, Los Angeles, CA, Oct. 15–17, 1985; Proceedings, Institute of Environmental Sciences, Mount Prospect, IL, 1986, pp. 40–44.

[7]Koons, H. C., "Summary of Environmentally Induced Electrical Discharges on the P78-2 (SCATHA) Satellite," *Journal of Spacecraft and Rockets*, Vol. 20, No. 5, 1983, pp. 425–431.

[8]Wilson, P. F., and Ma, M. T., "Fields Radiated by Electrostatic Discharges," *IEEE Transactions* on *Electromagnetic Compatibility*, Vol. 33, No. 1, 1991, pp. 10–18.

[9]Leung, P., and Plamp, G., "Characteristics of RF Resulting from Dielectric Discharges," *IEEE Transactions on Nuclear Science*, Vol. NS-29, No. 6, 1982, pp. 1610–1614.

Alfred L. Vampola
Associate Editor

Plasma Chamber Testing of Advanced Photovoltaic Solar Array Coupons

G. Barry Hillard*
NASA Lewis Research Center, Cleveland, Ohio 44135

Introduction

HISTORICALLY, power systems on U.S. spacecraft have operated at the nominal 28 V dc inherited from the aircraft industry, a choice made feasible by their typically small size and relatively low power requirements. As satellites and other spacecraft have steadily become larger, heavier, and more sophisticated, solar arrays and other power sources have begun to be operated at higher voltages to minimize the system currents. The major advantage of higher operating voltages is the lower mass of the cabling required to transmit electrical power from the power sources efficiently.

The advent of high-voltage systems poses a number of challenges to the spacecraft designer. In particular, the interaction of materials and systems with space plasma, negligible at 28 V, now becomes important. Materials and design practices which have been standard for low-voltage systems are susceptible to various plasma interactions and in some cases will prove unsuitable when high voltages are employed. The Solar Array Module Plasma Interactions Experiment (SAMPIE)'" is a Space Shuttle experiment designed to investigate and quantify these high-voltage plasma interactions.

Results from SAMPIE will play a key role in the design and construction of high-voltage space power systems. Among its various experiment samples, a number of solar cell coupons (representing design technologies of current interest) will be biased to high voltages to measure both arcing and plasma current collection. One of the principal objectives of the experiment is to test the performance of the Advanced Photovoltaic Solar Array (APSA).[4]

APSA is characterized principally by the use of very thin (60 μ) solar cells mounted on a flexible deployable blanket. The resulting array has very high specific power, exceeding 130 W/kg beginning of life (BOL) even using silicon solar cells. On SAMPIE, a flexible, deployable geometry is not practical and the cell coupon must be hard-mounted to a piece of aluminum. It was expected that the mounting scheme would have no impact on the plasma interactions SAMPIE is designed to test since all cells, interconnects, and bus bars are on the front side. A further assumption, valid at the traditional 28 V bus voltage, was that the material properties of the array blanket are not important to the electrical performance of the array. Since APSA arrays are now being designed using several blanket materials which are not strong electrical insulators, this assumption is questionable for high-voltage operation. To test the role of different blanket materials under high-voltage conditions, three twelve-cell prototype coupons of 2-cm by 4-cm silicon cells were constructed and tested in a space simulation chamber.

Received Feb. 16, 1993; revision received May 15, 1993; accepted for publication June 11, 1993.

*Physicist, Space Environment Effects Branch, MS 302-1. Member AIAA.

Sample Construction

Originally designed for deployment in geosynchronous Earth orbit (GEO), APSA initially used a flexible blanket of carbon-loaded Kapton® mounted in an external frame. The carbon-loaded material provides a blanket which is slightly conducting and serves as an active charge control measure in geostationary applications where spacecraft charging is the prime concern. The first test sample was therefore constructed on a 15.24-cm by 17.78-cm (6-in. by 7-in.) carbon-loaded Kapton blanket. The outer 1.27-cm (0.5-in.) perimeter was covered front and back with Kapton tape to increase mechanical strength leaving an active area of 12.7 cm by 15.24 cm (5 in. by 6 in.) of exposed carbon-loaded material. The solar cells were wired as three parallel strings each having four cells in series. The module was suspended from its four comers by four nonconducting bands in a frame made from nonconducting material.

A second coupon was constructed using standard Kapton-H, which we will henceforth refer to simply as "Kapton." The module was constructed on a 15.24-cm by 17.78-cm (6-in. by 7-in.) piece of Kapton which was then bonded to an aluminum substrate using a nonconductive adhesive. The aluminum substrate was anodized on the top and conversion coated on the back, rendering the top surface insulating and the bottom surface conducting. The effect of this is to electrically isolate the solar array from the underlying substrate. The coupon was wired as three parallel strings each having four cells in series.

The final coupon, more appropriate for use in low Earth orbit (LEO), has a blanket of germanium-coated Kapton for protection from atomic oxygen attack. The germanium coating provides a higher resistance than carbon loading but is still weakly conductive. Unlike the carbon-loaded material, for which conductivity is a bulk property, this material uses germanium as a thin film deposited on a substrate of Kapton. The cells were mounted on a piece of 12.7-cm by 15.24-cm (5-in. by 6-in.) Kapton with 150 nm of germanium coating on both sides. It was then bonded to an aluminum substrate as above and wired as a single-series string.

In all three cases, electrical wires were attached to the two busbars and shorted together to allow for the application of bias voltage. Exposed busbars are a major source of plasma current collection. All busbars were made from .32-cm- (1/8-in.) wide strips but differed slightly in length because of the different wiring schemes. General layout of the cells, spacing between them, and number, size, and placement of interconnects was as close to being the same for all three as possible. These properties are summarized in Table 1.

Test Facility and Procedures

Testing was done in the Plasma Interaction Facility (PIF) at the Lewis Research Center. All measurements were made in a space simulation chamber offering a cylindrical volume 1.8 m (6 ft) in diameter by 1.8 m long. A 91.4-cm (36-in.) diffusion pump provided an initial pumpdown to approximately 5×10^{-7} torr. Plasma was generated by a hollow cathode discharge source with a continuous flow of argon. Pressure in the tank during operation of the plasma source was approximately 5×10^{-5} torr.

An electrometer, a Keithley model 237, was used to apply a bias voltage to the test sample and measure the resulting collected current. Ion currents were measured with applied biases from 0 to −200 V in 10-V increments while electron currents were measured with applied biases from 0 to +600 V in 25-V increments. Ion and electron current collection sweeps were made separately, always beginning with zero volts bias